

Calbindin-D_{28K} dynamically controls TRPV5-mediated Ca²⁺ transport

Tim T Lambers¹, Frank Mahieu³, Elena Oancea⁴, Louis Hoofd¹, Frank de Lange², Arjen R Mensenkamp¹, Thomas Voets³, Bernd Nilius³, David E Clapham^{3,4}, Joost G Hoenderop¹ and René J Bindels^{1,*}

¹Department of Physiology, Radboud University Nijmegen Medical Centre, The Netherlands, ²Department of Cell Biology, Radboud University Nijmegen Medical Centre, The Netherlands, ³Department of Physiology, KU Leuven, Campus Gasthuisberg, Leuven, Belgium and ⁴Cardiovascular Department, HHMI, Children's Hospital and Department of Neurobiology, Harvard Medical School, USA

In Ca²⁺-transporting epithelia, calbindin-D_{28K} (CaBP_{28K}) facilitates Ca²⁺ diffusion from the luminal Ca²⁺ entry side of the cell to the basolateral side, where Ca²⁺ is extruded into the extracellular compartment. Simultaneously, CaBP_{28K} provides protection against toxic high Ca²⁺ levels by buffering the cytosolic Ca²⁺ concentration ([Ca²⁺]_i) during high Ca²⁺ influx. CaBP_{28K} consistently colocalizes with the epithelial Ca²⁺ channel TRPV5, which constitutes the apical entry step in renal Ca²⁺-transporting epithelial cells. Here, we demonstrate using protein-binding analysis, subcellular fractionation and evanescent-field microscopy that CaBP_{28K} translocates towards the plasma membrane and directly associates with TRPV5 at a low [Ca²⁺]_i. ⁴⁵Ca²⁺ uptake measurements, electrophysiological recordings and transcellular Ca²⁺ transport assays of lentivirus-infected primary rabbit connecting tubule/distal convolute tubule cells revealed that associated CaBP_{28K} tightly buffers the flux of Ca²⁺ entering the cell via TRPV5, facilitating high Ca²⁺ transport rates by preventing channel inactivation. In summary, CaBP_{28K} acts in Ca²⁺-transporting epithelia as a dynamic Ca²⁺ buffer, regulating [Ca²⁺]_i in close vicinity to the TRPV5 pore by direct association with the channel.

The EMBO Journal (2006) 25, 2978–2988. doi:10.1038/sj.emboj.7601186; Published online 8 June 2006

Subject Categories: membranes & transport

Keywords: Ca²⁺ homeostasis; kidney; TIRF; transient receptor potential; vitamin D

Introduction

The vitamin D-dependent Ca²⁺-binding proteins, named calbindins (CaBPs), are expressed in cells that are challenged by a high Ca²⁺ influx such as in brain, bone, teeth, inner ear,

*Corresponding author. Department of Physiology, Radboud University Nijmegen Medical Centre, Nijmegen Centre for Molecular Life Sciences, PO Box 9101, 6500 HB Nijmegen, The Netherlands.
Tel.: +31 24 3614211; Fax: +31 24 3616413;
E-mail: R.Bindels@ncmls.ru.nl

Received: 27 January 2006; accepted: 16 May 2006; published online: 8 June 2006

placenta, mammary gland, kidney and intestine. In these tissues, CaBPs (i.e., CaBP_{9K} and CaBP_{28K}) are widely regarded as a key component in cellular Ca²⁺ handling. In Ca²⁺-transporting epithelial cells, CaBPs display the potential to facilitate multiple steps in the process of transcellular Ca²⁺ transport. First, Ca²⁺ influx in these cells is mediated by the epithelial Ca²⁺ channels TRPV5 and TRPV6, which are distinct members of the transient receptor potential (TRP) family (Montell *et al*, 2002) acting as gatekeepers facilitating cellular Ca²⁺ entry due to a steep inward electrochemical gradient across the luminal membrane of epithelial cells (Hoenderop *et al*, 2005). The activity of these highly Ca²⁺-selective channels is tightly regulated by the Ca²⁺ concentration in close vicinity to the channel mouth (Hoenderop *et al*, 1999b). Thus, adequate buffering of Ca²⁺ is essential for a continuous influx of Ca²⁺ through these channels. Second, during high rates of transcellular Ca²⁺ transport, strict regulation of the intracellular Ca²⁺ concentration ([Ca²⁺]_i) is crucial in protecting the cell against the cytotoxic high levels of Ca²⁺ (Tymianski, 1996). Buffering of Ca²⁺ by specialized Ca²⁺-binding proteins is, therefore, required (Lukas and Jones, 1994; Pauls *et al*, 1996; Schwaller *et al*, 2002). Third, Ca²⁺ entering at the luminal side of the cell has to diffuse, without affecting other intracellular processes, to the basolateral side, where the Na⁺/Ca²⁺ exchanger (NCX1) and/or the plasma membrane ATPase (PMCA1b) extrude Ca²⁺ into the extracellular compartment. In transepithelial Ca²⁺ transport, CaBPs have been implicated in facilitated diffusion of Ca²⁺ from the luminal membrane to the basolateral surface by increasing the diffusional range of Ca²⁺ (Bronner and Stein, 1988; Bronner, 1989). Moreover, the importance of CaBPs in Ca²⁺-transporting epithelial cells is underlined by the consistent coexpression with the Ca²⁺ transport proteins including TRPV5, TRPV6, NCX1 and PMCA1b (Lambers *et al*, 2006).

Negative feedback regulation of channel activity by an increased [Ca²⁺]_i is not restricted to the epithelial Ca²⁺ channels. A broad range of both voltage- and non-voltage-operated ion channels are regulated by [Ca²⁺]_i (Kits and Mansvelter, 1996; Jones *et al*, 1999). Ion channels that are negatively regulated by Ca²⁺ inactivate upon a local rise in [Ca²⁺]_i in close proximity to the channel pore. Previous studies indicated that the Ca²⁺ sensor calmodulin is responsible for the Ca²⁺-dependent regulation of particularly voltage-operated Ca²⁺ channels (Zuhlke *et al*, 1999; DeMaria *et al*, 2001). However, how [Ca²⁺]_i near a channel pore is regulated is not well defined. Several studies implicate CaBPs in facilitated diffusion of Ca²⁺. However, other than mathematical models (Feher *et al*, 1992) and coordinated regulation of renal Ca²⁺ transport proteins (van Abel *et al*, 2005), limited experimental data are available to substantiate these hypotheses.

In addition, previous studies indicated that CaBP_{28K} acts as a cytosolic Ca²⁺ buffer to protect neurons against large fluctuations in [Ca²⁺]_i (Iacopino and Christakos, 1990; Lukas

and Jones, 1994; Guo *et al*, 1998). Here, the buffer capacity of $\text{CaBP}_{28\text{K}}$ affects the shape of the postsynaptic Ca^{2+} signals and may underlie paired pulse facilitation of synapses (Airaksinen *et al*, 1997; Blatow *et al*, 2003; Schmidt *et al*, 2003). Recently, it was shown in cerebellar Purkinje neurons that $\text{CaBP}_{28\text{K}}$ directly interacts with membrane-targeted inositol-1,4,5-trisphosphate and acts as a Ca^{2+} sensor to regulate the degradation of inositol messengers in an activity-dependent manner (Schmidt *et al*, 2005). Thus, $\text{CaBP}_{28\text{K}}$ displays several properties that imply an important role in Ca^{2+} -induced signal transmission and hence may function not only as a Ca^{2+} buffer, but also as a Ca^{2+} sensor affecting downstream processes in the cell.

A key biochemical property specifying a Ca^{2+} sensor is the presence of EF-hand motifs that undergo a conformational change upon Ca^{2+} binding. $\text{CaBP}_{28\text{K}}$ is equipped with six EF-hand motifs that bind Ca^{2+} in a highly cooperative fashion. First, Ca^{2+} binds to the high-affinity EF-hand site 1, followed by EF-hands 4 and 5 and finally EF-hand 3 is loaded with Ca^{2+} , in contrast to EF-hands 2 and 6, which do not bind Ca^{2+} (Venters *et al*, 2003). Although the crystal structure of $\text{CaBP}_{28\text{K}}$ has not been determined, structural analysis measured by nuclear magnetic resonance indicated that conformational changes occur in $\text{CaBP}_{28\text{K}}$ upon Ca^{2+} binding (Berggard *et al*, 2002; Venyaminov *et al*, 2004).

The aim of the present study was to determine how CaBPs contribute to the regulation of TRPV5 channel activity, intracellular Ca^{2+} handling and transcellular Ca^{2+} transport in epithelial cells. By a comprehensive approach using protein-binding analysis, live cell imaging and functional assays, this study reveals a crucial role of $\text{CaBP}_{28\text{K}}$ in TRPV5-mediated transepithelial Ca^{2+} transport in kidney. Here, we show that $\text{CaBP}_{28\text{K}}$ acts as a dynamic Ca^{2+} buffer regulating the local $[\text{Ca}^{2+}]_i$ in close vicinity to the TRPV5 pore by direct association with the channel.

Results

Concomitant regulation of calbindin- $D_{28\text{K}}$ and TRPV5 in kidney

In kidney, $\text{CaBP}_{28\text{K}}$ and TRPV5 colocalized in the distal convoluted tubule (DCT) and the connecting tubule (CNT) (Figure 1A). These cells transport Ca^{2+} transcellularly from the pro-urine to the blood compartment (Hoenderop *et al*, 2005). To investigate whether there is a correlation between the expression of TRPV5 and $\text{CaBP}_{28\text{K}}$, the abundance of these proteins was analyzed in different animal models that were treated with calciotropic hormones, exposed to various dietary Ca^{2+} levels or ablated for genes encoding Ca^{2+} transport proteins (Figure 1B). Importantly, a highly significant correlation between the TRPV5 expression and $\text{CaBP}_{28\text{K}}$ abundance was consistently observed. $\text{CaBP}_{28\text{K}}$ is predominantly localized along the apical side of TRPV5-expressing renal cells (Figure 1A). Therefore, the apical localization of $\text{CaBP}_{28\text{K}}$ was investigated in kidneys of TRPV5^{-/-} compared to wild-type mice. To this end, the immuno-positive staining of $\text{CaBP}_{28\text{K}}$ was semiquantified in five subcellular regions of DCT and CNT cells (Figure 1C). In TRPV5^{-/-} kidney, $\text{CaBP}_{28\text{K}}$ was equally distributed throughout the tubular cells with no apparent apical localization, whereas $\text{CaBP}_{28\text{K}}$ was significantly more abundant in the apical region in wild-type kidney

cells. This finding further substantiates that the apical localization of $\text{CaBP}_{28\text{K}}$ is dependent on the presence of TRPV5.

Calbindin- $D_{28\text{K}}$ interacts with TRPV5 in a Ca^{2+} -dependent manner

Ion channels in epithelial cells are frequently regulated by associated intracellular protein complexes. A potential interaction between $\text{CaBP}_{28\text{K}}$ and TRPV5 was investigated using GST pull-down assays. In addition, the interaction of $\text{CaBP}_{28\text{K}}$ with other TRPV members, including the highly homologous TRPV6 and closely related TRPV4 channels, was studied. $\text{CaBP}_{28\text{K}}$ bound to both the N- and C-termini of TRPV5 and TRPV6 in the absence of Ca^{2+} (5 mM EDTA), whereas the binding was virtually abolished in the presence of Ca^{2+} (1 mM CaCl_2) (Figure 1D). However, binding between $\text{CaBP}_{28\text{K}}$ and TRPV4 could not be detected either in the presence or absence of Ca^{2+} (data not shown). Subsequently, the interaction of TRPV5 and $\text{CaBP}_{28\text{K}}$ was evaluated by co-precipitation from GST- $\text{CaBP}_{28\text{K}}$ - and TRPV5-expressing human embryonic kidney (HEK293) cells. The Ca^{2+} dependency of this association was investigated by incubation of the cells with BAPTA-AM to decrease $[\text{Ca}^{2+}]_i$. To this end, cell lysates were incubated with glutathione-coupled Sepharose beads to precipitate GST- $\text{CaBP}_{28\text{K}}$ complexes and immunoblots containing the precipitated proteins were analyzed for the presence of TRPV5. TRPV5 co-precipitated with GST- $\text{CaBP}_{28\text{K}}$ in cells that were treated with BAPTA-AM, whereas the channel was not precipitated from non-treated cells (Figure 1E). In addition, co-precipitation of TRPV5 could not be detected in GST- and TRPV5-expressing cells, demonstrating the specificity of the $\text{CaBP}_{28\text{K}}$ association.

$\text{CaBP}_{28\text{K}}$ translocates towards the plasma membrane in a Ca^{2+} - and TRPV5-dependent manner

The physiological characteristics of the interaction of $\text{CaBP}_{28\text{K}}$ with TRPV5 suggests that this Ca^{2+} -binding protein translocates towards the plasma membrane at a low $[\text{Ca}^{2+}]_i$. This hypothesis was investigated by the isolation of plasma membrane-enriched fractions of TRPV5- and $\text{CaBP}_{28\text{K}}$ -transfected HeLa cells. As compared to the endogenously expressed Na,K-ATPase, $\text{CaBP}_{28\text{K}}$ was more abundant ($260 \pm 105\%$, $n = 3$, $P < 0.05$) in the plasma membrane-enriched fraction of cells that were treated with BAPTA-AM compared to non-treated cells (Figure 2A, left panel). Importantly, cells lacking TRPV5 did not reveal an elevated expression of $\text{CaBP}_{28\text{K}}$ in the plasma membrane-enriched fraction after BAPTA-AM treatment (Figure 2A, right panel). Subsequently, $\text{CaBP}_{28\text{K}}$ expression in plasma membrane-enriched fractions of primary rabbit CNT/cortical collecting duct (CNT/CCD) cultures endogenously expressing TRPV5 and $\text{CaBP}_{28\text{K}}$ (Hoenderop *et al*, 2005) was evaluated. In line with the experiments using transfected cells, $\text{CaBP}_{28\text{K}}$ was more abundant ($146 \pm 6\%$, $n = 3$, $P < 0.05$) in plasma membrane-enriched fractions of BAPTA-AM-treated primary CNT/CCD cultures as compared to non-treated cultures (Figure 2B).

Next, the Ca^{2+} -dependent translocation of $\text{CaBP}_{28\text{K}}$ towards the plasma membrane in TRPV5-expressing HEK293T cells was investigated by total internal reflection fluorescence (TIRF) or evanescent-field microscopy. TIRF microscopy illuminates fluorophores within 100–200 nm of the plasma membrane–glass cover slip interface, with

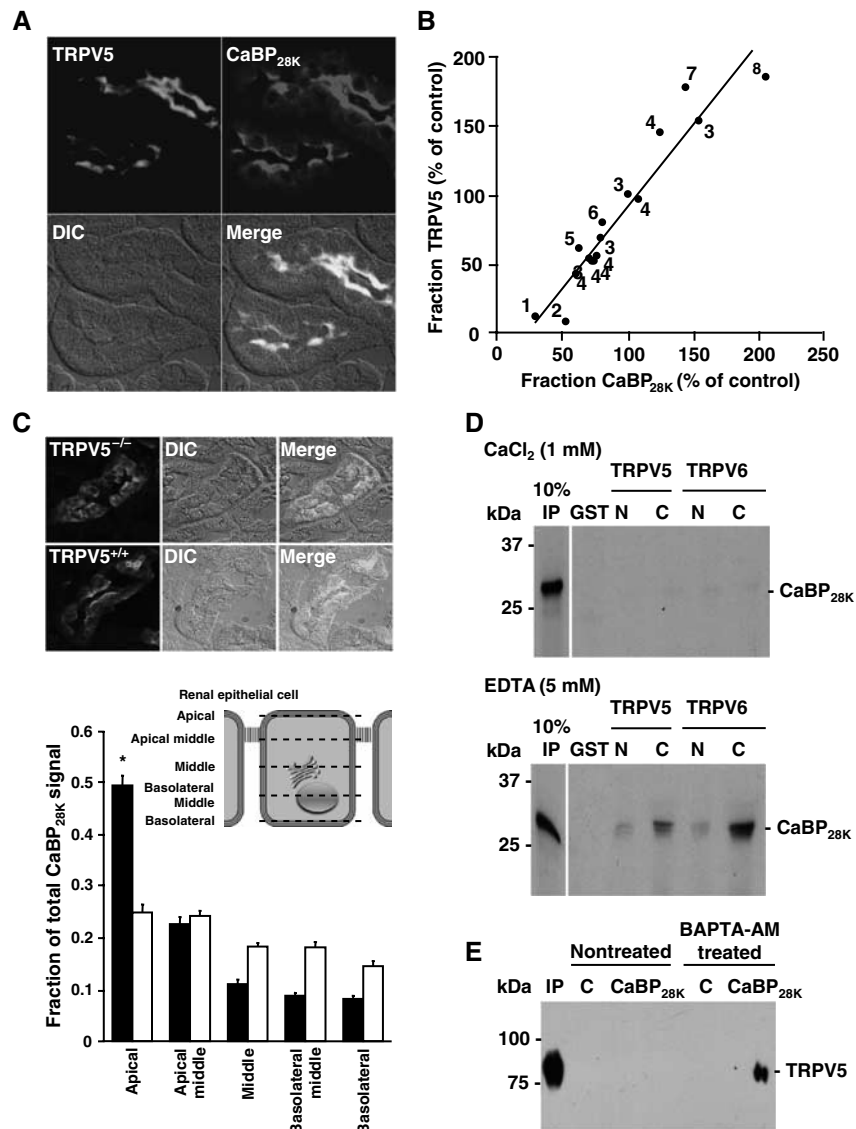


Figure 1 Coordinated expression and direct association of TRPV5 and CaBP_{28K}. **(A)** Colocalization of TRPV5 (green) and CaBP_{28K} (red) in the DCT and CNT. **(B)** Correlation in TRPV5 and CaBP_{28K} expression after treatment (¹parathyroidectomized (van Abel *et al*, 2005); ²tacrolimus (Nijenhuis *et al*, 2005); ³acidose/alkalose (Nijenhuis *et al*, 2006); ⁴thiazide (Nijenhuis *et al*, 2004, 2005); ⁵calcimimetics (van Abel *et al*, 2005); ⁶ovariectomized (van Abel *et al*, 2005); ⁷dexamethasone (Nijenhuis *et al*, 2004); ⁸ovariectomized + vitamine D₃ (van Abel *et al*, 2002)). R² = 0.9068. **(C)** Localization of CaBP_{28K} in kidney sections of TRPV5^{-/-} and wild-type mice. The epithelial cells were divided in different regions including apical, apical-middle, middle, basolateral-middle and basolateral as indicated. The immuno-positive CaBP_{28K} staining of these different cellular regions in 30 cells of six different tubules was calculated as described in Materials and methods. Significant differences in CaBP_{28K} intensities within the group are indicated by an asterisk. Open bars represent TRPV5^{-/-}, closed bars represent wild-type. **(D)** [³⁵S]Methionine-labeled, *in vitro*-translated CaBP_{28K} was incubated either in the presence (1 mM CaCl₂) or absence (5 mM EDTA) of Ca²⁺, with GST or GST fused to the N- or C-terminus of TRPV5 and TRPV6 immobilized on glutathione-Sepharose 4B beads. Input control (IP) represents 10% of the total pull-down input. **(E)** Cells were cotransfected with pEBG-CaBP_{28K} (GST-CaBP_{28K}) and pCIneo-TRPV5-IRES-EGFP or pEBG (GST) and pCIneo-TRPV5-IRES-EGFP (control, C). To decrease the [Ca²⁺]_i, cells were treated with BAPTA-AM. Lysates were loaded on glutathione-Sepharose 4B beads, and after extensive washing co-precipitation was investigated by immunoblotting using the guinea-pig anti-TRPV5 antibody (IP = input). The two TRPV5 immuno-positive bands correspond to the core (lower) and glycosylated forms of the protein.

excitation intensity depending on the relative indices of refraction and the angle of incidence. Light intensity falls exponentially in the axial (z) direction, such that fluorescence output is inversely proportional to the distance from the plasma membrane. TIRF therefore enabled us to study the dynamic process of CaBP_{28K} translocation towards the plasma membrane in a direction vertical to the plasma membrane, without interference of cytosolic CaBP_{28K} fluorescence. The presence of EYFP-CaBP_{28K} in the TIRF

signal of cells cotransfected with EYFP-CaBP_{28K} and TRPV5-EGFP was followed in the presence and absence of BAPTA-AM, respectively. After BAPTA-AM treatment, the EYFP-CaBP_{28K} TIRF signal increased in time as compared to non-treated cells (Figure 3A and B). In line with the cell fractionation experiments, this increase of EYFP-CaBP_{28K} TIRF signal was not observed in cells lacking TRPV5 (Figure 3C and D). Furthermore, the BAPTA-dependent changes in TIRF signal were not detected in cells expressing

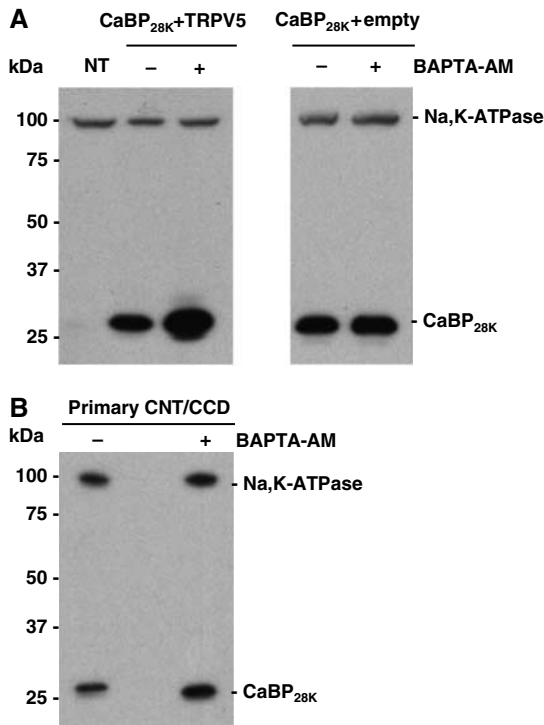


Figure 2 Subcellular localization of CaBP_{28K} at low intracellular Ca^{2+} concentrations. **(A)** Cells were transfected with CaBP_{28K} and TRPV5 (left panel) or CaBP_{28K} and empty vector (right panel) and treated with or without BAPTA-AM. Plasma membrane-enriched fractions were probed for the presence of endogenously expressed Na,K-ATPase and exogenously expressed CaBP_{28K} using anti-Na,K-ATPase and anti-CaBP_{28K} antibodies, respectively. NT = non-transfected. **(B)** Plasma membrane-enriched fractions of primary CNT/CCD cultures, either treated with or without BAPTA-AM, were isolated and probed for the presence of endogenously expressed CaBP_{28K} and Na,K-ATPase. Representative blots of three independent experiments are shown.

TRPV5-IRES-EGFP (bicistronic expression of TRPV5 and EGFP) (Figure 3E and F), demonstrating that the observed alterations in EYFP-CaBP_{28K} fluorescence represent a cellular redistribution of CaBP_{28K}.

Coexpression of CaBP_{28K} elevates $^{45}\text{Ca}^{2+}$ uptake in TRPV5-expressing MDCK cells

In order to investigate the functional role of the Ca^{2+} -binding EF-hand motifs in CaBP_{28K}, a Ca^{2+} -insensitive mutant (CaBP_{28K}ΔEF) was constructed and characterized by $^{45}\text{Ca}^{2+}$ overlay and pull-down experiments. As compared to the negative control (GST), disruption of the EF-hand motifs in GST-CaBP_{28K} resulted in a Ca^{2+} -insensitive CaBP_{28K} mutant, whereas wild-type GST-CaBP_{28K} displayed normal $^{45}\text{Ca}^{2+}$ binding (Figure 4A). In addition, pull-down analysis demonstrated that CaBP_{28K}ΔEF binds in the absence (5 mM EDTA) as well as presence (1 mM CaCl_2) of Ca^{2+} to the N- and C-terminus of both TRPV5 and TRPV6 (Figure 4B). To investigate whether CaBP_{28K}ΔEF competes with wild-type CaBP_{28K} for TRPV5 binding, increasing amounts of non-radioactive *in vitro*-translated CaBP_{28K}ΔEF were added during the pull-down assay. This resulted in a dose-dependent reduction of CaBP_{28K} binding, indicating that CaBP_{28K}ΔEF competed with wild-type CaBP_{28K} for TRPV5 association (Figure 4C).

The role of CaBP_{28K} and the Ca^{2+} -binding EF-hand motifs in CaBP_{28K} in TRPV5-mediated $^{45}\text{Ca}^{2+}$ uptake was assessed. To this end, stably transfected Madin-Darby Canine Kidney type-I epithelial (MDCK) cell lines were generated that express TRPV5 and CaBP_{28K} or CaBP_{28K}ΔEF. Total expression of EGFP-TRPV5 remained constant in the MDCK-TRPV5, MDCK-TRPV5-CaBP_{28K} and MDCK-TRPV5-CaBP_{28K}ΔEF cell lines (Figure 5A). Furthermore, immunoblot analysis demonstrated the integrity of the EGFP-TRPV5 fusion protein by the protein band of ~100 kDa. In addition, flow cytometry analysis of the EGFP signal was employed to investigate the percentage of EGFP-TRPV5-positive cells. Importantly, >98% of the cells expressed EGFP-TRPV5, indicating that virtually all cells contribute to $^{45}\text{Ca}^{2+}$ uptake in the MDCK-TRPV5, MDCK-TRPV5-CaBP_{28K} and MDCK-TRPV5-CaBP_{28K}ΔEF cell lines (Figure 5B). These results demonstrated that differences in $^{45}\text{Ca}^{2+}$ uptake are not owing to alterations in TRPV5 expression. Stable expression of EGFP-TRPV5 in MDCK cells (MDCK-TRPV5) resulted in an ~6-fold increase of ruthenium red-sensitive $^{45}\text{Ca}^{2+}$ uptake compared to empty vector-transfected cells (mock). Stable expression of CaBP_{28K} in these cells (MDCK-TRPV5-CaBP_{28K}) (Figure 5C) further increased the ruthenium red-sensitive $^{45}\text{Ca}^{2+}$ uptake by ~2-fold as compared to EGFP-TRPV5- and empty vector-expressing (MDCK-TRPV5-mock) cells (Figure 5D). Stable expression of CaBP_{28K}ΔEF in EGFP-TRPV5-expressing cells (MDCK-TRPV5-CaBP_{28K}ΔEF) did not result in an increase of ruthenium red-sensitive $^{45}\text{Ca}^{2+}$ uptake, indicating the importance of the Ca^{2+} -binding EF-hand motifs in CaBP_{28K}.

CaBP_{28K} has no effect on the current characteristics of TRPV5

As CaBP_{28K} binds to TRPV5 and possesses the ability to regulate downstream cellular processes, CaBP_{28K} could directly affect channel activity. The effect of CaBP_{28K} on the electrophysiological characteristics of TRPV5 was investigated by controlling $[\text{Ca}^{2+}]_i$ in a spatially uniform manner using uncaging of Ca^{2+} from the photolabile Ca^{2+} chelator DMNP-EDTA. TRPV5 activity in the presence and absence of CaBP_{28K} and CaBP_{28K}ΔEF was correlated to $[\text{Ca}^{2+}]_i$ (see Supplementary Figure S1 for additional information). Regulating $[\text{Ca}^{2+}]_i$ enabled us to study the effect of CaBP_{28K} on the characteristics of TRPV5 without the influence of Ca^{2+} buffering by CaBP_{28K}. Neither CaBP_{28K} nor CaBP_{28K}ΔEF modulated the Ca^{2+} sensitivity of TRPV5 when $[\text{Ca}^{2+}]_i$ was gradually increased from 100 to 600 nM (Figure 6A and B).

CaBP_{28K}ΔEF dominant-negatively inhibits transcellular Ca^{2+} transport in primary rabbit CNT/CCD cultures

If the translocation of CaBP_{28K} towards and subsequent interaction with TRPV5 is of any physiological relevance, disruption of the CaBP_{28K}-TRPV5 association will result in a decreased Ca^{2+} buffering at the entry gate and coherent impairment of transcellular Ca^{2+} transport. This hypothesis was experimentally evaluated by using the lentiviral expression system to express EGFP-CaBP_{28K}ΔEF in primary rabbit CNT/CCD cultures and subsequent Ca^{2+} transport measurements across these infected confluent cell monolayers. Viral expression of EGFP-CaBP_{28K}ΔEF resulted in a dominant-negative effect on transcellular Ca^{2+} transport across primary CNT/CCD cultures (Figure 7A). As compared to

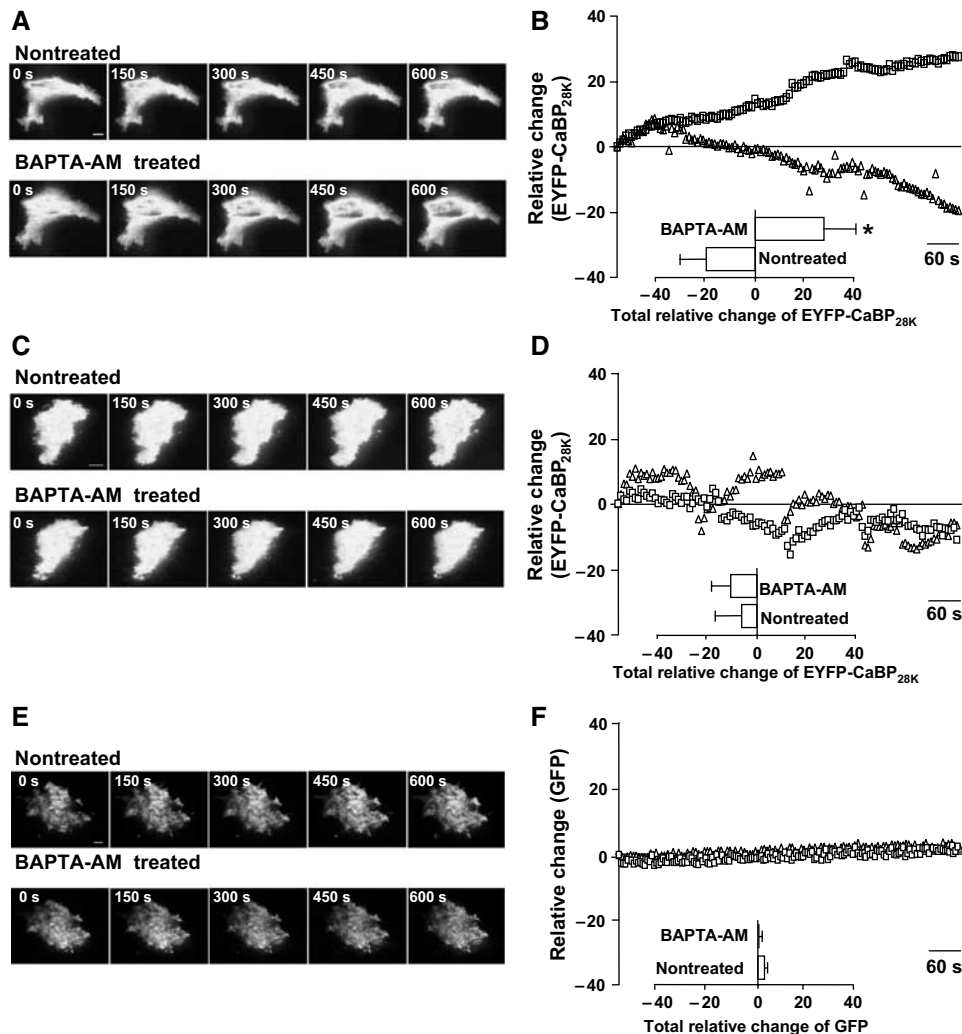


Figure 3 CaBP_{28K} translocation at low intracellular Ca^{2+} concentrations. (A) TIRF images of a single cell expressing EYFP-CaBP_{28K} and TRPV5-ECFP that was treated with (lower panel) or without (upper panel) BAPTA-AM. Scale bar = 5 μm . (B) Average time courses of the TIRF signal of EYFP-CaBP_{28K} in EYFP-CaBP_{28K}⁻ and TRPV5-ECFP-expressing cells that were treated either with (■) or without (Δ) BAPTA-AM ($n = 7$). Significant differences in total EYFP changes after BAPTA-AM treatment (inset) are indicated by an asterisk ($P < 0.05$). (C) TIRF images of a single cell expressing EYFP-CaBP_{28K} that was treated with (lower panel) or without (upper panel) BAPTA-AM. Scale bar = 5 μm . (D) Average time courses of the TIRF signal of EYFP-CaBP_{28K}-expressing cells that were treated either with (■) or without (Δ) BAPTA-AM ($n = 5$). (E) TIRF images of single cells expressing TRPV5-IRES-EGFP treated with (lower panel) or without (upper panel) BAPTA-AM. Scale bar = 5 μm . (F) Average time courses of the TIRF signal in TRPV5-IRES-EGFP-expressing cells that were treated either with (■) or without (Δ) BAPTA-AM ($n = 5$). In all images, a gradient filter was applied such that saturation of TIRF fluorescence turns red and the intensities were measured between 5 and 10% of the visible ‘footprint’ of the cell.

non-infected cultures, viral expression of only EGFP did not influence transcellular Ca^{2+} transport. Viral infection with efficiencies of $\sim 50\%$ (Supplementary Figure S2) did not affect the transepithelial resistance in any of the conditions tested, confirming the integrity of the CNT/CCD monolayer (data not shown). Importantly, only half of the CNT/CCD cells expressed the CaBP_{28K} ΔEF mutant, indicating that the observed inhibition is significantly underestimated. To investigate whether CaBP_{28K} ΔEF inhibited TRPV5-mediated transcellular Ca^{2+} transport in primary CNT/CCD cultures, the potent TRPV5 channel blocker ruthenium red was included during the Ca^{2+} transport assay. Addition of 10 μM ruthenium red to the apical side of the cell monolayer abolished transcellular Ca^{2+} transport in the absence or presence of exogenous CaBP_{28K} ΔEF (Figure 7A).

Next, we measured expression of wild-type CaBP_{28K} and EGFP-CaBP_{28K} ΔEF in these primary renal cell cultures

(Figure 7B). No differences in wild-type CaBP_{28K} expression were detected between EGFP- and EGFP-CaBP_{28K} ΔEF -infected cells as compared to the endogenously expressed Na,K-ATPase, indicating that the observed effects were not due to downregulation of endogenous CaBP_{28K}.

Discussion

The present study identified CaBP_{28K} as a dynamic Ca^{2+} buffer facilitating TRPV5-mediated Ca^{2+} transport by buffering $[\text{Ca}^{2+}]_i$ in close vicinity to the channel mouth. This conclusion is based on the following observations. First, CaBP_{28K} translocates towards TRPV5-containing plasma membranes upon a decrease in $[\text{Ca}^{2+}]_i$. Second, CaBP_{28K} directly associates with TRPV5 at a low $[\text{Ca}^{2+}]_i$. Third, expression of CaBP_{28K} in TRPV5-expressing cells increases TRPV5-mediated Ca^{2+} influx, whereas inactivation of the

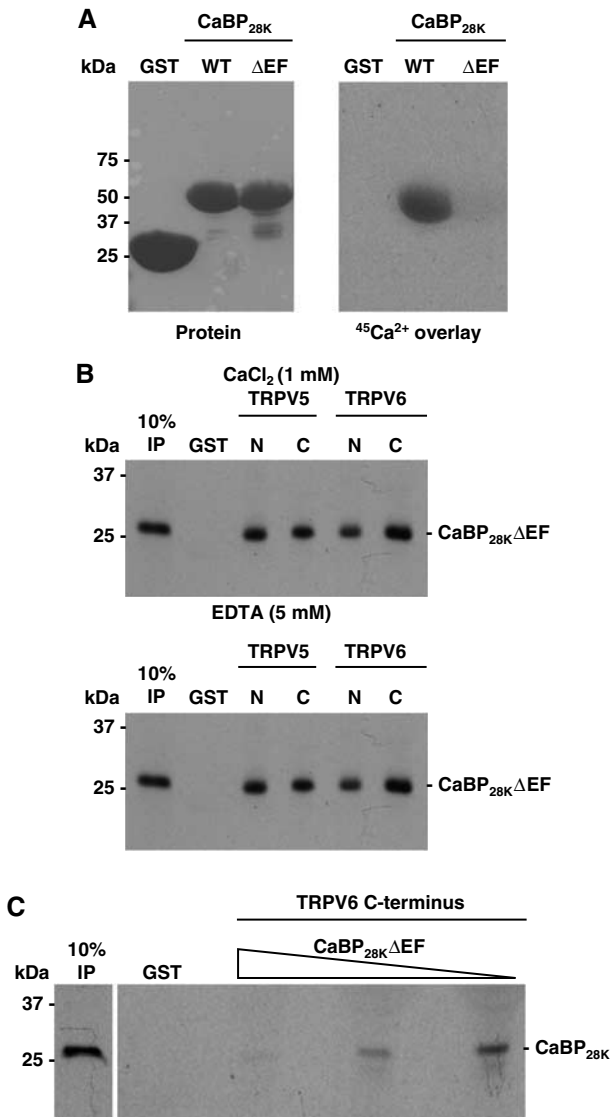


Figure 4 Characterization of a Ca^{2+} -insensitive $\text{CaBP}_{28\text{K}}$ mutant. (A) Wild-type $\text{CaBP}_{28\text{K}}$ and $\text{CaBP}_{28\text{K}}\Delta\text{EF}$ were fused to GST (left panel) and $^{45}\text{Ca}^{2+}$ binding was determined (right panel). (B) [^{35}S]Methionine-labeled, *in vitro*-translated $\text{CaBP}_{28\text{K}}\Delta\text{EF}$ was incubated either in the presence (1 mM CaCl_2) or absence (5 mM EDTA) of Ca^{2+} , with GST or GST fused to the N- and C-termini of TRPV5 and TRPV6 immobilized on glutathione-Sepharose 4B beads. Input control (IP) represents 10% of the total pull-down input. (C) [^{35}S]Methionine-labeled *in vitro*-translated $\text{CaBP}_{28\text{K}}\Delta\text{EF}$ was incubated in the presence of increasing amounts of non-radioactive *in vitro*-translated $\text{CaBP}_{28\text{K}}\Delta\text{EF}$ with GST or GST fused to the C-termini of TRPV5 immobilized on glutathione-Sepharose 4B beads. This pull-down experiment was performed in the absence of Ca^{2+} (5 mM EDTA). Input control (IP) represents 10% of the input.

EF-hand motifs in $\text{CaBP}_{28\text{K}}$ abolishes this stimulatory effect. Fourth, the Ca^{2+} -insensitive $\text{CaBP}_{28\text{K}}$ mutant ($\text{CaBP}_{28\text{K}}\Delta\text{EF}$) competes with wild-type $\text{CaBP}_{28\text{K}}$ for TRPV5 association, resulting in a dominant-negative inhibition of transepithelial Ca^{2+} transport in primary rabbit CNT/CCD cultures.

In the past, $\text{CaBP}_{28\text{K}}$ was identified as a high-capacity Ca^{2+} buffer with Ca^{2+} affinities fitting the classical properties of a Ca^{2+} buffer. However, sequential Ca^{2+} binding and conformational changes suggested that $\text{CaBP}_{28\text{K}}$ can act as a Ca^{2+} sensor controlling downstream cellular processes (Gross

et al, 1987; Winsky and Kuznicki, 1995; Berggard *et al*, 2002; Venyaminov *et al*, 2004). $\text{CaBP}_{28\text{K}}$ is highly expressed in Ca^{2+} -transporting epithelia where it colocalizes with TRPV5. This study reveals that the expressions of $\text{CaBP}_{28\text{K}}$ and TRPV5 are positively correlated, suggesting a fundamental role of $\text{CaBP}_{28\text{K}}$ in the regulation of TRPV5 activity. In various studies exploring the regulatory role of the calcitropic hormones including vitamin D, estrogens, parathyroid hormone and dietary Ca^{2+} , we observed the concomitant regulation of TRPV5 and $\text{CaBP}_{28\text{K}}$ in kidney (Lambers *et al*, 2006). Likewise, genetic ablation of TRPV5 in mice resulted in a decreased expression of $\text{CaBP}_{28\text{K}}$ (Hoenderop *et al*, 2003). Blockage of TRPV5 by ruthenium red eliminated parathyroid hormone-stimulated transepithelial Ca^{2+} transport in primary CNT/CCD cultures and simultaneously decreased the expression of $\text{CaBP}_{28\text{K}}$. The magnitude of the Ca^{2+} influx through TRPV5 predominantly controlled the expression of $\text{CaBP}_{28\text{K}}$ (van Abel *et al*, 2005). Interestingly, Arnold and Heintz (1997) identified a 40-bp element in the $\text{CaBP}_{28\text{K}}$ promoter that forms a cell-specific and Ca^{2+} -sensitive transcriptional regulatory mechanism that may play a key role in setting the Ca^{2+} buffering capacity of Purkinje cells (Arnold and Heintz, 1997). Together, these data assure adequate $\text{CaBP}_{28\text{K}}$ expression to facilitate sufficient buffering of the TRPV5-mediated Ca^{2+} influx.

Here, we demonstrated that in Ca^{2+} -transporting epithelia, $\text{CaBP}_{28\text{K}}$ also directly associates with TRPV5 in a Ca^{2+} -dependent fashion. In line with this interaction, in kidney cells $\text{CaBP}_{28\text{K}}$ is found in the cytosol as well as along the apical membrane, where it colocalizes with TRPV5. This apical localization of $\text{CaBP}_{28\text{K}}$ is significantly disturbed in kidney cells of $\text{TRPV5}^{-/-}$ mice where $\text{CaBP}_{28\text{K}}$ is distributed evenly throughout the cytosol. In addition, both static and dynamic measurements using cells coexpressing $\text{CaBP}_{28\text{K}}$ and TRPV5 revealed that $\text{CaBP}_{28\text{K}}$ accumulates at the plasma membrane when $[\text{Ca}^{2+}]_i$ is low. Importantly, this translocation only occurs in the presence of TRPV5. Taken together, these data suggest that $\text{CaBP}_{28\text{K}}$ possesses the ability to specifically target to TRPV5-expressing plasma membranes at a low $[\text{Ca}^{2+}]_i$. $\text{CaBP}_{28\text{K}}$ translocation is supported by previous findings showing that a fraction of $\text{CaBP}_{28\text{K}}$ specifically associates with particular subcellular domains (Hubbard and McHugh, 1995; Winsky and Kuznicki, 1995) and that $\text{CaBP}_{28\text{K}}$ redistributes after Ca^{2+} sensing (Nemere *et al*, 1991). Further evidence for targeted $\text{CaBP}_{28\text{K}}$ mobility has been provided by Schmidt *et al* (2005), who demonstrated a specific association of $\text{CaBP}_{28\text{K}}$ with membrane-associated inositol-1,4,5-triphosphate, but not with cytosolic inositol-1,4,5-triphosphate.

In addition to $\text{CaBP}_{28\text{K}}$, other Ca^{2+} -binding proteins were found to associate with and affect the activity of TRPV5 via distinct mechanisms. Functional expression of TRPV5 requires binding of the S100A10-annexin 2 complex, whereas 80K-H acts as a Ca^{2+} sensor regulating TRPV5 activity (van de Graaf *et al*, 2003; Gkika *et al*, 2004). Regulation by the ubiquitous calmodulin, however, seems to be restricted to the closely related family member TRPV6 (Lambers *et al*, 2004). This multifaceted regulation of TRPV5 enables a strict control of transcellular Ca^{2+} transport at the apical entry gate. It is, however, not clear yet how these Ca^{2+} -binding proteins integrate in this complex regulatory network to balance TRPV5-mediated Ca^{2+} influx.

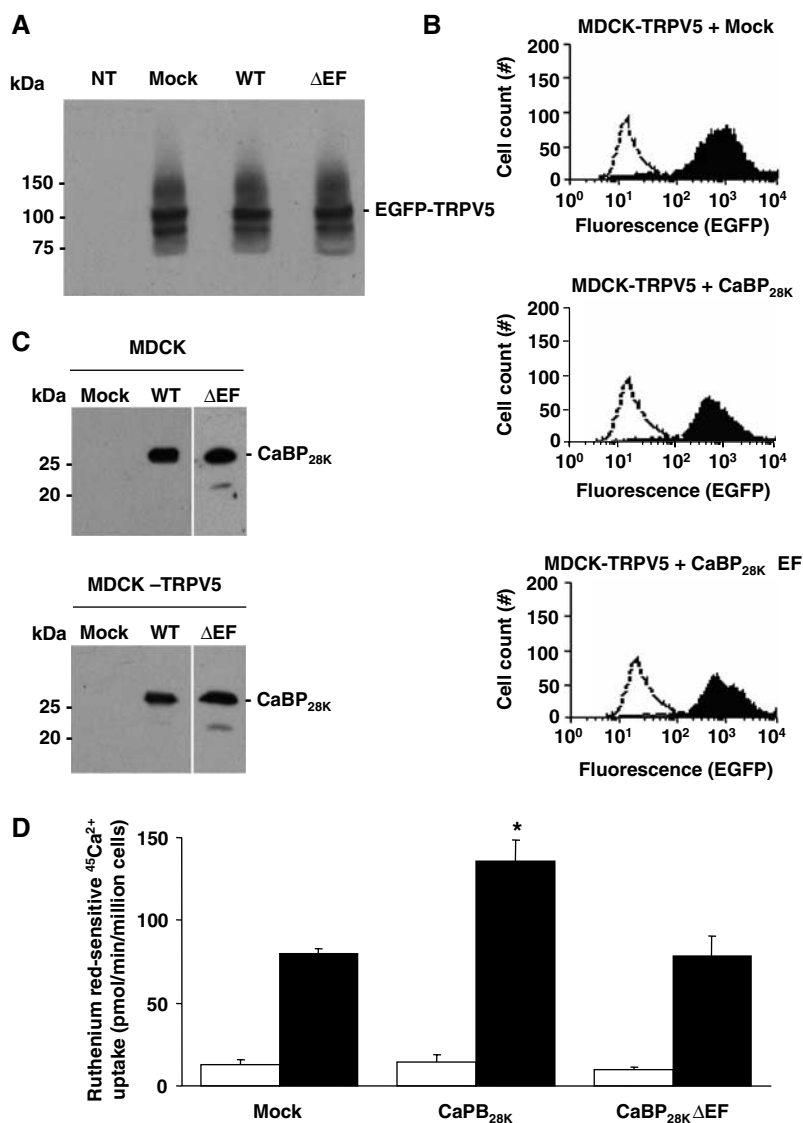


Figure 5 Role of CaBP_{28K} in TRPV5-mediated $^{45}\text{Ca}^{2+}$ uptake. EGFP-TRPV5 and CaBP_{28K}, CaBP_{28K}ΔEF or empty vector were stably expressed in MDCK cells. The expression level of EGFP-tagged TRPV5 as determined using rabbit anti-GFP antibody (A) or flow cytometry analysis (B; black peaks) reveals that the expression of TRPV5 in empty vector- and CaBP_{28K}-expressing cells is equal. The open peak in the three panels indicates background fluorescence in non-transfected cells. The two TRPV5 immuno-positive bands correspond to the core (lower) and glycosylated forms of EGFP-TRPV5. (C) The stable expression of CaBP_{28K} and CaBP_{28K}ΔEF in MDCK cells or MDCK cells expressing EGFP-TRPV5 was verified using anti-CaBP_{28K} antibodies. (D) Ruthenium red-sensitive $^{45}\text{Ca}^{2+}$ uptake of MDCK cells stably expressing both (black bars) TRPV5 and CaBP_{28K}, CaBP_{28K}ΔEF or empty vector and MDCK cells stably expressing (open bars) CaBP_{28K}, CaBP_{28K}ΔEF or empty vector. Significant differences in $^{45}\text{Ca}^{2+}$ uptake are indicated by an asterisk ($P < 0.05$).

Coexpression of CaBP_{28K} in TRPV5-expressing HEK293 cells increased the Ca^{2+} uptake, whereas inactivation of the EF-hand motifs in CaBP_{28K} blocked this stimulatory effect. CaBP_{28K}ΔEF was still able to bind TRPV5, although the Ca^{2+} dependency of the association was abolished. This implies that binding of CaBP_{28K} to TRPV5 does not directly affect the physiological properties of TRPV5, otherwise the presence of Ca^{2+} -insensitive CaBP_{28K} would also lead to an increase in TRPV5-mediated Ca^{2+} uptake. Furthermore, this emphasizes the importance of the EF-hand motifs in CaBP_{28K}. The activity of TRPV5 is tightly regulated by $[\text{Ca}^{2+}]_i$ in such a way that Ca^{2+} entering through TRPV5 exerts a negative feedback on channel activity (Hoenderop *et al*, 1999b). The present data showing Ca^{2+} -dependent association of TRPV5 and CaBP_{28K} and an elevated $^{45}\text{Ca}^{2+}$ uptake in TRPV5 and

CaBP_{28K} coexpressing cells suggests that the increase in $^{45}\text{Ca}^{2+}$ uptake is due to CaBP_{28K} Ca^{2+} buffering in close vicinity of the channel mouth. The activity of TRPV5 in the presence of CaBP_{28K} or CaBP_{28K}ΔEF was measured at various, experimentally controlled, $[\text{Ca}^{2+}]_i$ to further investigate whether CaBP_{28K} directly affects TRPV5 current characteristics. In response to a gradual increase of $[\text{Ca}^{2+}]_i$ by UV-induced uncaging of Ca^{2+} , the activity of TRPV5 decreased, revealing the negative feedback of Ca^{2+} on channel activity. Coexpression of CaBP_{28K} or CaBP_{28K}ΔEF did not change these observations, indicating that CaBP_{28K} does not directly affect channel inactivation characteristics at controlled $[\text{Ca}^{2+}]_i$. Thus, CaBP_{28K} associates with TRPV5 and stimulates TRPV5-mediated Ca^{2+} influx by increasing the buffering of $[\text{Ca}^{2+}]$ in close proximity to the channel mouth. This

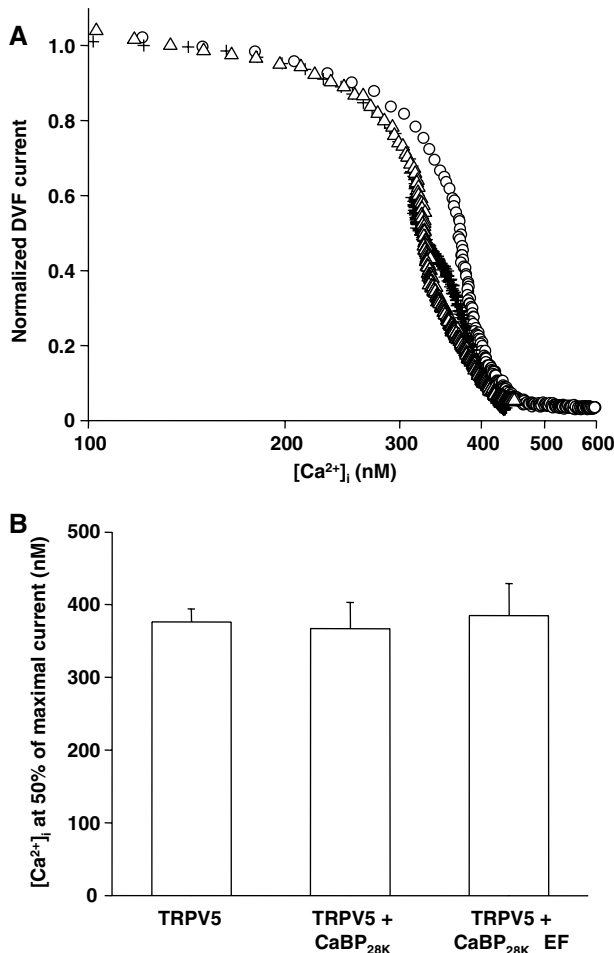


Figure 6 Direct influence of CaBP_{28K} on the characteristics of TRPV5. (A) Dose–response curves showing the effect of an increasing $[\text{Ca}^{2+}]_i$ on the normalized Na^+ inward current in divalent-free extracellular solution (DVF) of cells expressing TRPV5 (O, $n=9$), TRPV5 and CaBP_{28K} (+, $n=11$) or TRPV5 and CaBP_{28K}ΔEF (Δ, $n=12$). (B) Averaged IC_{50} for each of the transfections and recordings shown in panel A.

dynamic buffering and association is a unique process in comparison to channel regulation by other Ca^{2+} -binding proteins like calmodulin. Channel-associated calmodulin senses $[\text{Ca}^{2+}]_i$ and regulates channel activity by directly affecting channel (in)activation (Zuhlke *et al*, 1999; DeMaria *et al*, 2001).

Association of CaBP_{28K} with TRPV5 and the consequent local buffering of Ca^{2+} is essential to facilitate the process of transcellular Ca^{2+} transport, which is evident from the dominant-negative effect of CaBP_{28K}ΔEF on transcellular Ca^{2+} transport in primary CNT/CCD cultures. CaBP_{28K}ΔEF lacks Ca^{2+} buffering capacity, but competes with endogenous CaBP_{28K} for binding sites on TRPV5, as revealed by the reduction of CaBP_{28K} and TRPV5 association in the presence of CaBP_{28K}ΔEF. This will reduce the local buffering of Ca^{2+} entering the epithelial cell via TRPV5, which subsequently results in inactivation of the channel and reduced transcellular transport rates. Note that addition of ruthenium red abolished transcellular Ca^{2+} transport in the absence or presence of exogenous CaBP_{28K}ΔEF. Thus, these findings demonstrate that CaBP_{28K} regulates TRPV5-mediated Ca^{2+} transport.

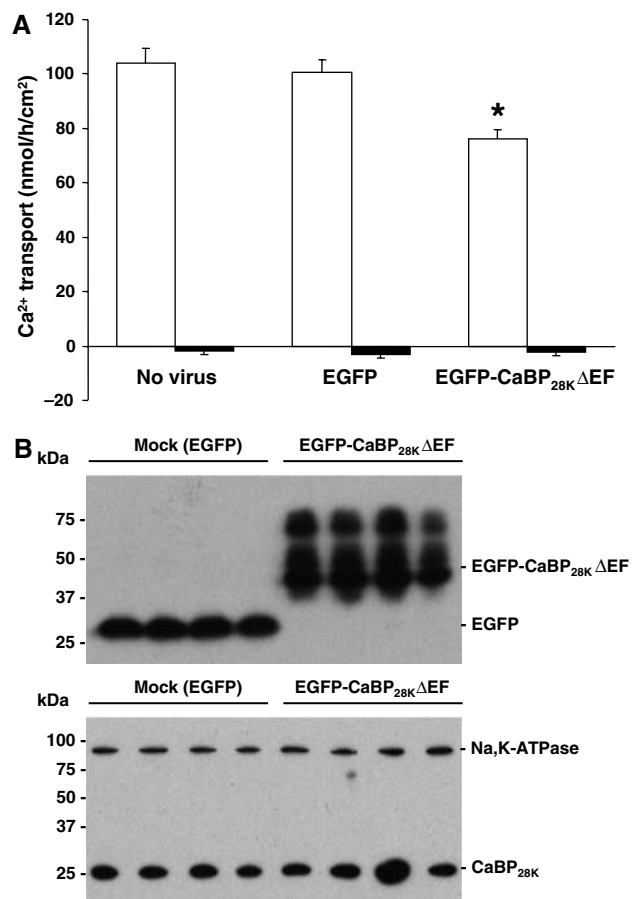


Figure 7 Effect of CaBP_{28K}ΔEF on transcellular Ca^{2+} transport. (A) Effect of lentivirus-mediated overexpression of GFP and GFP-CaBP_{28K}ΔEF on transcellular Ca^{2+} transport in primary rabbit CNT/CCD cells. Averaged transcellular Ca^{2+} transport for each infection is expressed as mean \pm s.e.m. A 10 μM portion of ruthenium red was added to the apical side of the cell monolayer during the transport assay to estimate the TRPV5-mediated Ca^{2+} transport. Significant differences as compared to mock-infected cells are indicated by an asterisk ($P < 0.05$). (B) The expression of GFP and GFP-CaBP_{28K}ΔEF (upper panel) was assessed with immunoblotting using rabbit anti-GFP antibody and the expression of endogenous CaBP_{28K} was checked with monoclonal anti-CaBP_{28K} antibody that does not recognize GFP-CaBP_{28K}ΔEF (lower panel). To check for equal loading, the expression of the endogenously expressed Na,K-ATPase was measured (lower panel).

Our previous findings that during transcellular Ca^{2+} transport in renal epithelial cells no apparent changes in the overall $[\text{Ca}^{2+}]_i$ could be detected (Koster *et al*, 1995) indicate that overall Ca^{2+} buffering is efficiently controlled in these cells. These measurements were, however, not performed on the subcellular level or in close proximity to the channel mouth where $[\text{Ca}^{2+}]$ fluctuates during transcellular Ca^{2+} transport. Opening of epithelial Ca^{2+} channels likely elicits Ca^{2+} influx of such a large magnitude that spatial distribution of Ca^{2+} is complicated by insufficient local Ca^{2+} buffers as suggested for voltage-operated Ca^{2+} channels (Neher, 1998). The dominant-negative effect of CaBP_{28K}ΔEF on transcellular Ca^{2+} transport in primary CNT/CCD cultures, however, revealed that a channel-associated Ca^{2+} buffer is of utmost importance for buffering of the Ca^{2+} influx through TRPV5.

Together, these findings constitute the first direct evidence that CaBP_{28K} is essential for transepithelial Ca^{2+} transport

and elucidate the molecular role of CaBP_{28K} as a dynamic Ca²⁺ buffer. At a low [Ca²⁺]_i, CaBP_{28K} translocates towards the plasma membrane and associates with TRPV5. Here, it buffers Ca²⁺ that enters the cell via TRPV5, thereby counteracting local accumulation of cytosolic free Ca²⁺ and coherent inactivation of the channel. Upon Ca²⁺ binding, CaBP_{28K} diffuses from TRPV5 and subsequently facilitates transport of Ca²⁺ to the basolateral membrane. Furthermore, this illustrates an intrinsic mechanism of targeted Ca²⁺ buffering by spatial interactions to subcellular domains where local Ca²⁺ levels become detrimental. Probably, similar mechanisms occur in brain, bone, teeth, inner ear, placenta and intestine where CaBPs are abundantly expressed and where cells tolerate large fluctuations in [Ca²⁺]_i.

Materials and methods

Molecular biology

TRPV4, 5 and 6 N- and C-termini were cloned into the pGEX6p-2 vector (Amersham Pharmacia Biotech, Roosendaal, The Netherlands). TRPV5 was cloned into the pCINeo/IRES-EGFP expression vector as described (Nilius *et al*, 2002) and fused to the C-terminus of EGFP or ECFP by subcloning into pEGFP-C1 and pECFP (Clontech, Palo Alto, CA). CaBP_{28K} was cloned into the *Xenopus laevis* oocyte expression vector pT7Ts and pEBG (Tanaka *et al*, 1995), pGEX6p-2 and pCINeo/IRES-EGFP expression vectors using PCR. An EYFP-CaBP_{28K} fusion construct was generated by cloning CaBP_{28K} into pEYFP-C1 (Clontech, Palo Alto, CA) and a Ca²⁺-insensitive CaBP_{28K} mutant (CaBP_{28K}ΔEF) was constructed by mutating the EF-hand motifs (EF1: D24A, D26A; EF2: D69A, D70A; EF3: D111A, D113A, E119A, E121A, E122A; EF4: D155A, D159A, E163A, E166A; EF5: D212A, D217A, E220A; EF6: D251A). All constructs were verified by sequence analysis and the integrity of the fusion constructs was investigated by Western blot analysis using a rabbit anti-GFP antibody.

Cell culture

HEK293, HEK293T, HeLa and MDCK cells were grown and transfected as described (Lambers *et al*, 2004). MDCK cells stably expressing both EGFP-TRPV5 and CaBP_{28K} were constructed as previously described (van de Graaf *et al*, 2006) and maintained in medium containing 800 μg/ml G418/700 μg/ml hygromycin (GIBCO Europe, Breda, The Netherlands). Expression was verified using mouse or rabbit anti-CaBP_{28K} (Sigma-Aldrich, Zwijndrecht, The Netherlands) and rabbit anti-GFP antibodies, respectively. Five cell line clones were pooled to eliminate differences between independent clones. For flow cytometry analysis of EGFP-TRPV5 expression, relative fluorescence intensity was measured on a FACSCalibur™ (BD Biosciences, Amsterdam, The Netherlands). Primary cultures of rabbit CNT/CCD were isolated and transepithelial Ca²⁺ transport was measured as described previously (Hoenderop *et al*, 1999a).

Protein-binding analysis

GST pull-down assays with [³⁵S]methionine-labeled proteins in TBS-HCl pH 7.4 containing 0.5% (v/v) NP-40 and 1 mM Ca²⁺ or 5 mM EDTA were performed as described (Lambers *et al*, 2004). For binding competition assays, increasing amounts of non-radioactive *in vitro*-translated CaBP_{28K}ΔEF were included during the pull-down experiment of CaBP_{28K} and TRPV5.

HEK293 cells were transiently cotransfected with pEBG-CaBP_{28K} and pCINeo-TRPV5-IRES-EGFP. Cells were loaded with or without 50 μM BAPTA-AM for 30 min at 37°C and lysed by incubation for 1 h on ice in TBS pH 7.4 containing 0.5% (v/v) NP-40, 5 mM EDTA and the protease inhibitors leupeptin (0.01 mg/ml), pepstatin (0.05 mg/ml), phenylmethylsulfonyl fluoride (1 mM) and aprotinin (5 mg/ml). The lysates were centrifuged for 30 min at 16000 g and supernatants were incubated with glutathione Sepharose beads (Amersham Bioscience, Piscataway, NJ) for 16 h. After extensive washing in lysis buffer, co-precipitation was performed by immunoblot analysis using guinea-pig anti-TRPV5 (Hoenderop *et al*, 1999b).

Cell fractionation assay

Primary renal CNT/CCD cultures and transiently CaBP_{28K}- and TRPV5-transfected HeLa cells were homogenized in fractionation buffer (300 mM sucrose, 25 mM imidazole-HCl pH 7.4, 5 mM EDTA and protease inhibitors leupeptin (0.01 mg/ml), pepstatin (0.05 mg/ml), phenylmethylsulfonyl fluoride (1 mM) and aprotinin (5 mg/ml)). After centrifugation for 5 min at 4000 g 4°C to remove intact cells, nuclei and mitochondria, the supernatant was centrifuged at 16000 g 4°C. The plasma membrane-enriched pellet fraction was subjected to SDS-PAGE and immunoblots were analyzed with rabbit anti-CaBP_{28K} and rabbit anti-Na,K-ATPase (Hoenderop *et al*, 1999b) antibodies. The intensity of immuno-positive bands was measured and changes in the CaBP_{28K} signal were expressed as a ratio of the internal control Na,K-ATPase.

Confocal, TIRF microscopy and image analysis

For TRPV5 and CaBP_{28K} colocalization, a Zeiss LSM510meta (Carl Zeiss GmbH, Jena, Germany) confocal laser scanning microscope was used. Images were taken with a PlanApoChromatic 63 × 1.4 oil immersion DIC lens (Carl Zeiss GmbH, Jena, Germany). The cytosolic localization of CaBP_{28K} was quantified using Image J (NIH) software. Renal epithelial cells were divided in five regions (apical, apical-middle, middle, basolateral-middle and basolateral) and the intensities of the individual regions in 30 renal cells of six different tubules were calculated according to the following equation:

$$\text{relative intensity} = I_x / (I_{\text{apical}} + I_{\text{apicalmiddle}} + I_{\text{middle}} + I_{\text{basolateralmiddle}} + I_{\text{basolateral}})$$

where I_x is the intensity of domain X, I_{apical} is the apical intensity, $I_{\text{apical-middle}}$ is the apical-middle intensity, I_{middle} is the middle intensity, $I_{\text{basolateral-middle}}$ is the basolateral-middle intensity and $I_{\text{basolateral}}$ is the basolateral intensity.

To image EYFP-CaBP_{28K} in EYFP-CaBP_{28K}- and ECFP-TRPV5-transfected HEK293T cells, a custom-built objective-based TIRF microscope was used (Bezzlerides *et al*, 2004). Briefly, a 488 nm solid-state diode laser (Coherent, Santa Clara, CA) was focused onto a single-mode optical fiber (Newport, Irvine, CA) with a 5-axis fiber-coupler (New Focus, San Jose, CA) and guided through the rear illumination port of an Olympus IX70 fluorescence microscope. The laser light reflected from a specially coated dichroic mirror (Z488RDC; Chroma Technology, Rockingham, VT) passes through a high-numerical aperture objective (NA 1.45, ×60, Olympus, Melville, NY) and was totally internally reflected by the glass-water interface ($n = 1.37$). Fluorescence emitted from tagged proteins passed through an HQ515-30 m (Chroma) filter for EGFP/EYFP before being collected by a cooled CCD (ORCA ER II; Hamamatsu, Bridgewater, NJ). All imaging acquisition was performed with MetaMorph (Universal Imaging, West Chester, PA). Cells grown on glass coverslips were placed in a custom chamber with standard external solution (135 mM NaCl, 5 mM KCl, 1.5 mM MgCl₂, 1.5 mM CaCl₂, 20 mM HEPES, 10 mM D-glucose, pH 7.4 with HCl) and imaged at room temperature. Cells were screened for the expression of ECFP-TRPV5 and EYFP-CaBP_{28K} using the normal light fluorescence setup before switching to TIRF for EYFP imaging. Cells were analyzed for 10 min (1 frame/5 s) to establish a baseline in whole-cell TIRF measurements before 50 μM BAPTA-AM was added. After 15 min, to allow BAPTA loading of the cells, cells were again followed for 10 min (1 frame/5 s). To quantify changes in TIRF, intensities of the regions of interests of several ($n = 5-7$) cells, with areas between 5 and 10% of the visible 'footprint' of the cell, were averaged and normalized according to the following equation:

$$\text{relative change} = I(t) - I(0)$$

where $I(0)$ is the intensity at the beginning of the time series and $I(t)$ is the intensity at time point t .

⁴⁵Ca²⁺ binding and uptake assay

GST-CaBP_{28K} and GST were expressed and purified according to the manufacturers' protocol (Amersham Biosciences, Piscataway, NJ). Blots were washed in overlay-buffer (10 mM imidazole-HCl pH 7.4, 60 mM KCl, 0.5 mM MgCl₂) before incubation with ⁴⁵CaCl₂ (1 μCi/ml) in overlay-buffer. After extensive washing in 50% (v/v) ethanol and drying of the blots, bound ⁴⁵Ca²⁺ was determined by autoradiography. ⁴⁵Ca²⁺ uptake was determined using confluent layers of MDCK cells as described (den Dekker *et al*, 2005). To block

TRPV5-mediated $^{45}\text{Ca}^{2+}$ uptake, cells were incubated with $10\ \mu\text{M}$ ruthenium red.

Electrophysiology

Whole-cell currents in HEK293 cells transiently transfected with TRPV5 and $\text{CaBP}_{28\text{K}}$ were measured using an EPC-9 patch-clamp amplifier and Pulse software (HEKA Elektronik, Lambrecht, Germany). Monovalent cation currents were measured in divalent-free extracellular solution containing $150\ \text{mM}$ NaCl, $10\ \text{mM}$ EDTA and $10\ \text{mM}$ HEPES–NaOH, pH 7.4. The internal (pipette) solution contained $120\ \text{mM}$ NaCl, $1\ \text{mM}$ CaCl_2 , $20\ \text{mM}$ HEPES–NaOH and $1\ \text{mM}$ Fura-2, supplemented with $5\ \text{mM}$ 1-(4,5-methoxy-2-nitrophenyl)1,2-aminoethane-*N,N,N',N'*-tetraacetic acid (DMNP-EDTA). DMNP-EDTA is a Ca^{2+} chelator that exhibits a high affinity for Ca^{2+} ions with an increase in its K_d for Ca^{2+} upon photolysis (K_d rises from $5\ \text{nM}$ to $3\ \text{mM}$). All experiments were performed at room temperature. Current–voltage relationships were measured from linear 400-ms voltage ramps, from -100 to $+100\ \text{mV}$. Ramps were applied every 5 s from a holding potential of $+20\ \text{mV}$ with a sampling interval of 0.8 ms. All current amplitudes in the dose-response curves were normalized to values of the inward current at $-80\ \text{mV}$ and an intracellular Ca^{2+} concentration ($[\text{Ca}^{2+}]_i$) of $135\ \text{nM}$ and subsequently fitted with a Hill function (Origin 7.0 software, OriginLab Corporation, Northampton, MA). For photolytic release of Ca^{2+} and measurement of $[\text{Ca}^{2+}]_i$ during patch-clamp, Fura-2 was excited with light alternated between 350 and 380 nm using a monochromator (Polychrome IV, TILL Photonics, Planegg, Germany), and the resulting fluorescent signal was measured using a photodiode. The ratio of the fluorescent signal was converted into $[\text{Ca}^{2+}]_i$ values according to the Grynkiewicz equation (Grynkiewicz *et al*, 1985). Increases in $[\text{Ca}^{2+}]_i$ were achieved by increasing the duration of 350/380 nm illumination from 15 to 150 ms each.

Lentiviral infection of primary rabbit CNT/CCD cultures

Third-generation lentiviruses were produced by cotransfection of the packaging vectors pRSV-Rev, pMDL g/p RRE and pMD2G (from

Tronolab, Lausanne, Switzerland) into HEK293T cells as described (Dull *et al*, 1998). The virus titer was determined by p24 HIV ELISA (Murex Diagnostics, Dartford, UK). Primary rabbit CNT/CCD cultures were infected with lentiviruses containing EGFP or EGFP- $\text{CaBP}_{28\text{K}\Delta\text{EF}}$ immediately before plating in the presence of polybrene ($8\ \mu\text{g}/\text{ml}$) using 20 virus particles per cell (20 MOI). Virus was removed after 24 h and subsequently transepithelial Ca^{2+} transport was measured 6 days after infection in the presence of $10\ \mu\text{M}$ forskolin as described previously (Hoenderop *et al*, 1999a).

Statistical analysis

In all experiments, the data are expressed as mean \pm s.e.m. Overall statistical significance was determined by analysis of variance followed by Bonferroni to investigate individual significance. *P*-values below 0.05 were considered significant.

Supplementary data

Supplementary data are available at *The EMBO Journal* Online.

Acknowledgements

We thank Mr J Israel and Mrs S van Gessel for excellent experimental assistance, and Dr J Hoeven (LUMC Leiden, The Netherlands) and Dr D Trono (Lausanne, Switzerland) for providing lentiviral vectors. This work was supported by the Dutch Organization of Scientific Research (Zon-Mw 016.006.001, NWO-ALW 805.09.042), Human Frontiers Science Program (RGP32/2004), the Dutch Kidney Foundation (C03.6017) and the Onderzoeksraad KU Leuven (GOA 2004/07, FWO G.0214.99, FWO G.0136.00, FWO G.0172.03, Interuniversity Poles of Attraction Program, Prime Ministers Office IUAP). A work visit of Mr TT Lambers to the lab of Dr D Clapham was further supported by a grant of the van Walree Fund from the Royal Dutch Academy of Sciences.

References

- Airaksinen MS, Eilers J, Garaschuk O, Thoenen H, Konnerth A, Meyer M (1997) Ataxia and altered dendritic calcium signaling in mice carrying a targeted null mutation of the calbindin $\text{D}_{28\text{K}}$ gene. *Proc Natl Acad Sci USA* **94**: 1488–1493
- Arnold DB, Heintz N (1997) A calcium responsive element that regulates expression of two calcium binding proteins in Purkinje cells. *Proc Natl Acad Sci USA* **94**: 8842–8847
- Berggard T, Miron S, Onnerfjord P, Thulin E, Akerfeldt KS, Enghild JJ, Akke M, Linse S (2002) Calbindin $\text{D}_{28\text{K}}$ exhibits properties characteristic of a Ca^{2+} sensor. *J Biol Chem* **277**: 16662–16672
- Bezzzerides VJ, Ramsey IS, Kotecha S, Greka A, Clapham DE (2004) Rapid vesicular translocation and insertion of TRP channels. *Nat Cell Biol* **6**: 709–720
- Blatow M, Caputi A, Burnashev N, Monyer H, Rozov A (2003) Ca^{2+} buffer saturation underlies paired pulse facilitation in calbindin- $\text{D}_{28\text{K}}$ -containing terminals. *Neuron* **38**: 79–88
- Bronner F (1989) Renal calcium transport: mechanisms and regulation—an overview. *Am J Physiol* **257**: F707–F711
- Bronner F, Stein WD (1988) CaBP facilitates intracellular diffusion for Ca^{2+} pumping in distal convoluted tubule. *Am J Physiol* **255**: F558–F562
- DeMaria CD, Soong TW, Alseikhan BA, Alvania RS, Yue DT (2001) Calmodulin bifurcates the local Ca^{2+} signal that modulates P/Q-type Ca^{2+} channels. *Nature* **411**: 484–489
- den Dekker E, Schoeber J, Topala CN, van de Graaf SF, Hoenderop JG, Bindels RJ (2005) Characterization of a Madin–Darby canine kidney cell line stably expressing TRPV5. *Pflugers Arch* **450**: 236–244
- Dull T, Zufferey R, Kelly M, Mandel RJ, Nguyen M, Trono D, Naldini L (1998) A third-generation lentivirus vector with a conditional packaging system. *J Virol* **72**: 8463–8471
- Fehér JJ, Fullmer CS, Wasserman RH (1992) Role of facilitated diffusion of calcium by calbindin in intestinal calcium absorption. *Am J Physiol* **262**: C517–C526
- Gkika D, Mahieu F, Nilius B, Hoenderop JG, Bindels RJ (2004) 80K-H as a new Ca^{2+} sensor regulating the activity of the epithelial Ca^{2+} channel transient receptor potential cation channel V5 (TRPV5). *J Biol Chem* **279**: 26351–26357
- Gross MD, Nelsestuen GL, Kumar R (1987) Observations on the binding of lanthanides and calcium to vitamin D-dependent chick intestinal calcium-binding protein. Implications regarding calcium-binding protein function. *J Biol Chem* **262**: 6539–6545
- Grynkiewicz G, Poenie M, Tsien RY (1985) A new generation of Ca^{2+} indicators with greatly improved fluorescence properties. *J Biol Chem* **260**: 3440–3450
- Guo Q, Christakos S, Robinson N, Mattson MP (1998) Calbindin- $\text{D}_{28\text{K}}$ blocks the proapoptotic actions of mutant presenilin 1: reduced oxidative stress and preserved mitochondrial function. *Proc Natl Acad Sci USA* **95**: 3227–3232
- Hoenderop JG, Nilius B, Bindels RJ (2005) Calcium absorption across epithelia. *Physiol Rev* **85**: 373–422
- Hoenderop JG, Vaandrager AB, Dijkink L, Smolenski A, Gambaryan S, Lohmann SM, de Jonge HR, Willems PH, Bindels RJ (1999a) Atrial natriuretic peptide-stimulated Ca^{2+} reabsorption in rabbit kidney requires membrane-targeted, cGMP-dependent protein kinase type II. *Proc Natl Acad Sci USA* **96**: 6084–6089
- Hoenderop JG, van der Kemp AW, Hartog A, van de Graaf SF, van Os CH, Willems PH, Bindels RJ (1999b) Molecular identification of the apical Ca^{2+} channel in 1,25-dihydroxyvitamin D_3 -responsive epithelia. *J Biol Chem* **274**: 8375–8378
- Hoenderop JG, van Leeuwen JP, van der Eerden BC, Kersten FF, van der Kemp AW, Merillat AM, Waarsing JH, Rossier BC, Vallon V, Hummler E, Bindels RJ (2003) Renal Ca^{2+} wasting, hyperabsorption, and reduced bone thickness in mice lacking TRPV5. *J Clin Invest* **112**: 1906–1914
- Hubbard MJ, McHugh NJ (1995) Calbindin- $\text{D}_{28\text{K}}$ and calbindin- $\text{D}_{30\text{K}}$ (calretinin) are substantially localised in the particulate fraction of rat brain. *FEBS Lett* **374**: 333–337
- Iacopino AM, Christakos S (1990) Corticosterone regulates calbindin- $\text{D}_{28\text{K}}$ mRNA and protein levels in rat hippocampus. *J Biol Chem* **265**: 10177–10180

- Jones LP, DeMaria CD, Yue DT (1999) N-type calcium channel inactivation probed by gating-current analysis. *Biophys J* **76**: 2530–2552
- Kits KS, Mansvelder HD (1996) Voltage gated calcium channels in molluscs: classification, Ca²⁺ dependent inactivation, modulation and functional roles. *Invert Neurosci* **2**: 9–34
- Koster HP, Hartog A, Van Os CH, Bindels RJ (1995) Calbindin-D_{28K} facilitates cytosolic calcium diffusion without interfering with calcium signaling. *Cell Calcium* **18**: 187–196
- Lambers TT, Bindels RJ, Hoenderop JG (2006) Coordinated control of renal Ca²⁺ handling. *Kidney Int* **69**: 650–654
- Lambers TT, Weidema AF, Nilius B, Hoenderop JG, Bindels RJ (2004) Regulation of the mouse epithelial Ca²⁺ channel TRPV6 by the Ca²⁺-sensor calmodulin. *J Biol Chem* **279**: 28855–28861
- Lukas W, Jones KA (1994) Cortical neurons containing calretinin are selectively resistant to calcium overload and excitotoxicity *in vitro*. *Neuroscience* **61**: 307–316
- Montell C, Birnbaumer L, Flockerzi V, Bindels RJ, Bruford EA, Caterina MJ, Clapham DE, Harteneck C, Heller S, Julius D, Kojima I, Mori Y, Penner R, Prawitt D, Scharenberg AM, Schultz G, Shimizu N, Zhu MX (2002) A Unified Nomenclature for the Superfamily of TRP Cation Channels. *Mol Cell* **9**: 229–231
- Neher E (1998) Vesicle pools and Ca²⁺ microdomains: new tools for understanding their roles in neurotransmitter release. *Neuron* **20**: 389–399
- Nemere I, Leathers VL, Thompson BS, Luben RA, Norman AW (1991) Redistribution of calbindin-D_{28k} in chick intestine in response to calcium transport. *Endocrinology* **129**: 2972–2984
- Nijenhuis T, Hoenderop JG, Bindels RJ (2004) Downregulation of Ca²⁺ and Mg²⁺ transport proteins in the kidney explains tacrolimus (FK506)-induced hypercalciuria and hypomagnesemia. *J Am Soc Nephrol* **15**: 549–557
- Nijenhuis T, Renkema KY, Hoenderop JG, Bindels RJ (2006) Acid-base status determines the renal expression of Ca²⁺ and Mg²⁺ transport proteins. *J Am Soc Nephrol* **17**: 617–626
- Nijenhuis T, Vallon V, van der Kemp AW, Loffing J, Hoenderop JG, Bindels RJ (2005) Enhanced passive Ca²⁺ reabsorption and reduced Mg²⁺ channel abundance explains thiazide-induced hypocalciuria and hypomagnesemia. *J Clin Invest* **115**: 1651–1658
- Nilius B, Prenen J, Hoenderop JG, Vennekens R, Hoefs S, Weidema AF, Droogmans G, Bindels RJ (2002) Fast and slow inactivation kinetics of the Ca²⁺ channels ECaC1 and ECaC2 (TRPV5 and 6): role of the intracellular loop located between transmembrane segment 2 and 3. *J Biol Chem* **277**: 30852–30858
- Pauls TL, Cox JA, Berchtold MW (1996) The Ca²⁺-binding proteins parvalbumin and oncomodulin and their genes: new structural and functional findings. *Biochim Biophys Acta* **1306**: 39–54
- Schmidt H, Schwaller B, Eilers J (2005) Calbindin-D_{28K} targets myo-inositol monophosphatase in spines and dendrites of cerebellar Purkinje neurons. *Proc Natl Acad Sci USA* **102**: 5850–5855
- Schmidt H, Stiefel KM, Racay P, Schwaller B, Eilers J (2003) Mutational analysis of dendritic Ca²⁺ kinetics in rodent Purkinje cells: role of parvalbumin and calbindin-D_{28K}. *J Physiol* **551**: 13–32
- Schwaller B, Meyer M, Schiffmann S (2002) ‘New’ functions for ‘old’ proteins: the role of the calcium-binding proteins calbindin-D_{28K}, calretinin and parvalbumin, in cerebellar physiology. Studies with knockout mice. *Cerebellum* **1**: 241–258
- Tanaka M, Gupta R, Mayer BJ (1995) Differential inhibition of signaling pathways by dominant-negative SH2/SH3 adapter proteins. *Mol Cell Biol* **15**: 6829–6837
- Tymianski M (1996) Cytosolic calcium concentrations and cell death *in vitro*. *Adv Neurol* **71**: 85–105
- van Abel M, Hoenderop JG, Dardenne O, St-Arnaud R, van Os C, Van Leeuwen JP, Bindels RJ (2002) 1,25(OH)₂D₃-independent stimulatory effect of estrogen on the expression of ECaC1 in kidney. *J Am Soc Nephrol* **13**: 2102–2109
- van Abel M, Hoenderop JG, van der Kemp AW, Friedlaender MM, van Leeuwen JP, Bindels RJ (2005) Coordinated control of renal Ca²⁺ transport proteins by parathyroid hormone. *Kidney Int* **68**: 1708–1721
- van de Graaf SF, Chang Q, Mensenkamp AR, Hoenderop JG, Bindels RJ (2006) Direct interaction with Rab11a targets the epithelial Ca²⁺ channels TRPV5 and TRPV6 to the plasma membrane. *Mol Cell Biol* **26**: 303–312
- van de Graaf SF, Hoenderop JG, Gkika D, Lamers D, Prenen J, Rescher U, Gerke V, Staub O, Nilius B, Bindels RJ (2003) Functional expression of the epithelial Ca²⁺ channels (TRPV5 and TRPV6) requires association of the S100A10-annexin 2 complex. *EMBO J* **22**: 1478–1487
- Venters RA, Benson LM, Craig TA, Bagu J, Paul KH, Kordys DR, Thompson R, Naylor S, Kumar R, Cavanagh J (2003) The effects of Ca²⁺ binding on the conformation of calbindin D_{28K}: a nuclear magnetic resonance and microelectrospray mass spectrometry study. *Anal Biochem* **317**: 59–66
- Venyaminov SY, Klimtchuk ES, Bajzer Z, Craig TA (2004) Changes in structure and stability of calbindin-D_{28K} upon calcium binding. *Anal Biochem* **334**: 97–105
- Winsky L, Kuznicki J (1995) Distribution of calretinin, calbindin-D_{28K}, and parvalbumin in subcellular fractions of rat cerebellum: effects of calcium. *J Neurochem* **65**: 381–388
- Zuhlke RD, Pitt GS, Deisseroth K, Tsien RW, Reuter H (1999) Calmodulin supports both inactivation and facilitation of L-type calcium channels. *Nature* **399**: 159–162